Inverse Problems in Laminar Boundary-Layer Flows Over a Cylinder and a Sphere

P. Saikrishnan[a], S. Roy[b] and Prabir Daripa[c,*]

[a]Center for Industrial Mathematics, National University of Singapore, Singapore-117543

[b]Department of Mathematics, IIT Madras, Chennai- 600 036, India

[c]Department of Mathematics, Texas A&M University, College Station, Texas 77843-3368, USA

Abstract

The problem of recovery of the distribution of wall pressure gradient from the shear stress over a body surface in laminar boundary-layer flows is considered. This inverse problem when formulated using boundary-layer equations leads to a boundary value problem for a partial differential equation containing the unknown pressure gradient distribution as a coefficient. This coefficient is then found from the prescription of shear stress distribution along the body surface. In the direct problem, boundary-layer equations are solved to obtain the wall shear stress distribution from prescribed pressure gradient distribution along the body surface.

In this paper, inverse problems in laminar boundary-layer flows past an infinite circular cylinder and a sphere are solved using an invariant imbedding algorithm. The governing boundary-layer equations past these body surfaces are first solved numerically to obtain the wall shear stress distributions from known wall pressure distributions. With the computed wall shear stress distribution as an input data, the inverse problem is formulated by treating the pressure distribution as an unknown parameter. The proposed invariant imbedding technique is used to recover the unknown pressure distribution of inverse problem and the results are found to be in excellent agreement with the exact values.

Keywords: Inverse problems, Laminar boundary-layer flows, Invariant imbedding method,

*Author for correspondence (E-mail: Prabir.Daripa@math.tamu.edu).

1 Introduction

In boundary-layer flows, a class of problems deals with the determination of wall shear stress (or some other quantities of interest such as momentum thickness) from known wall pressure distribution. In keeping with the tradition, we call such problems direct problems in boundary-layer flows. Then there is another class of problems where the goal is to determine the distribution of wall pressure gradient from prescribed wall shear stress distribution. Again in keeping with tradition, we call these problems inverse problems in boundary-layer flows. Such inverse problems naturally arise from a variety of considerations, one such consideration being the need to reduce drag by controlling boundary layer separation.

There are flows, characterized by the geometry of the domain as well as boundary and initial conditions, in which the boundary layer remains attached to the body surface without separation. Such flows we will call attached flows. Then there are flows in which the boundary layer separates either to create a large wake or to attach back to the surface creating a small or a large bubble. Such flows we will call separated flows. In separated flows net drag usually increases substantially, an undesirable effect. Therefore it is usually desirable in some flows to control the separation of boundary layer either by delaying or by completely eliminating such separation. One of the ways to do this is to prescribe a desirable smooth distribution of shear stress along the body surface that will allow control of the separation point since zero shear stress occurs at a separation point. Then the task is to determine the distribution of wall pressure gradient that will yield the prescribed sheart stress distribution. Therefore inverse problems in boundary flows as discussed above are so important, specially in the context of controling separation of boundary-layer . Once this inverse problem is solved, of course, the task is to find a way to achieve such a wall pressure distribution which is not the subject of this paper. Nonetheless, it is worth mentioning that perhaps such desirable surface pressure distributions should be taken into account right at the outset to design surface profiles. In fact, this is another type of inverse problem in potential flows which has been much discussed by Daripa et. al. ([4],[5]) among many others.

There are various numerical methods for solving inverse problems in laminar boundary-layer flows. This inverse problem when formulated using boundary-layer equations leads to a boundary value problem for a partial differential equation containing the unknown pressure gradient distribution as a coefficient. This coefficient is then found from the prescription of shear stress distribution along the body surface. There are no known analytical methods for doing this. Therefore, numerical methods have been used to solve such problems. In this connection, it is worth mentioning the finite-difference method, so called the box-scheme, used by Keller and Cebeci [1] and an improved shooting technique in combination with the fourth order Runge-Kutta method employed by Horton ([2],[3]). The invariant imbedding approach which is also applicable to solving inverse problems in boundary-layer flows has not been applied to-date to test the method's robustness to solving such problems, and more so when the boundary-layer flow is non-planar. Presenting and adapting an invariant imbedding method for solving inverse problems as well as testing the performance of the method for such non-planar boundary-layer flows are the primary goals of this paper. Once this is settled in the affirmative, the method can be extended for various other situations in boundary-layer flows such as for boundary-layer flows past bodies of varying curvature, and for turbulent boundary-layer flows,

In this paper we present an invariant imbedding approach to solving inverse problems in boundary-layer flows past a cylinder and a sphere. We first solve direct problems for boundary-layer flows past a cylinder and a sphere to obtain distribution of wall shear stress from a prescription of wall pressure distribution for each of these bodies. Then, using the known distribution of wall shear stress in each of these cases the inverse problem in the boundary-layer is solved using an invariant imbedding approach to determine the pressure distribution which is found to be in excellent agreement with prescribed values in the direct problem in each of these two cases.

The paper is organized as follows. In section 2, the relevant equations for laminar boundary-layer flows are presented in various canonical forms which are then solved for boundary-layer flows over an infinite circular cylinder and a sphere. Numerical solutions of these direct problems yield the the distributions of shear stress over these bodies which are presented in this section. Section 3 presents inverse boundary-layer calculation procedure using an invariant imbedding approach to recover the surface pressure distributions from the distributions of surface shear stress obtained in section 2 from solving the direct problems. Numerical results obtained by implementation of this inverse method are presented and compared with exact known results in this section. Finally we conclude in section 4.

2 Formulation and Direct Problems

We consider steady laminar incompressible boundary-layer flows over a two-dimensional body (cylinder) or an axi-symmetric body (sphere) (See Figure 1). Let x and y be the curvilinear coordinates along and perpendicular to the body surface, respectively. Let u and v be the corresponding velocity components. The contour of the body of revolution is specified by

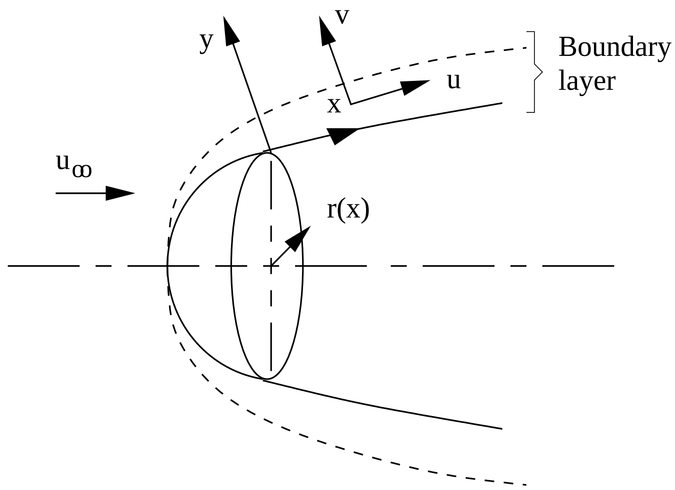

Figure 1: Figure 1: Flow model and coordinate system

the radii $r(x)$ of the section perpendicular to the axis. Neglecting the effect of transverse curvature, the governing boundary-layer continuity and momentum equations [9] are given by

$$(r^j u)_x + (r^j v)_y = 0, \tag{1}$$

$$u u_x + v u_y = u_e (u_e)_x + \nu u_{yy}, \tag{2}$$

and the boundary conditions are given by

$$u(x,0) = 0, \qquad v(x,0) = 0, \qquad u(x,\infty) = u_e(x).$$

Above ν is the kinematic viscosity, $u_e(x)$ is the velocity at the edge of the boundary layer, subscripts x and y denote the partial derivatives with respect to these variables respectively, subscript j is 0 or 1 according to whether the flow is two-dimensional or axi-symmetric. The following transformations

$$\xi = \int_0^x \left(\frac{u_e}{u_\infty}\right)\left(\frac{r}{R}\right)^{2j} d\left(\frac{x}{R}\right), \qquad \eta = \left(\frac{Re}{2\xi}\right)^{1/2}\left(\frac{u_e}{u_\infty}\right)\left(\frac{r}{R}\right)^{j}\left(\frac{y}{R}\right),$$

$$\psi(x,y) = \sqrt{2\mu R u_\infty \xi}\; f(\xi,\eta), \qquad u = \left(\frac{R}{r}\right)^j \frac{\partial\psi}{\partial y}, \qquad v = -\left(\frac{R}{r}\right)^j \frac{\partial\psi}{\partial x},$$

$$Re = \frac{u_\infty R}{\nu}, \qquad f_\eta = \frac{u(x)}{u_e(x)},$$

reduce the system of partial differential equations (1)-(2) to a canonical non-dimensional form

$$f_{\eta\eta\eta} + f f_{\eta\eta} + \beta(1 - f_\eta^2) = 2\xi(f_\eta f_{\eta\xi} - f_\xi f_{\eta\eta}). \tag{3}$$

Here ξ and η are transformed coordinates, ψ and f are the dimensional and dimensionless stream functions respectively, Re is the Reynolds number, R refers to the radius of the circular cylinder as well as that of the sphere, β $(= \frac{2\xi}{u_e}\frac{du_e}{d\xi})$ is the pressure gradient distribution, and subscripts ξ and η denote partial derivatives with respect to these variables respectively. The boundary conditions reduce to

$$f(\xi,0) = 0, \qquad f_\eta(\xi,0) = 0, \qquad f_\eta(\xi,\eta_\infty) = 1, \tag{4}$$

where η_∞ is the edge of the boundary layer. Equation (3) with conditions (4) can be solved numerically if $\beta(\xi)$ and $u_e(\xi)$, which depend on the shape of the body, are prescribed. In particular, we have obtained solutions in steady laminar incompressible boundary-layer flows over a cylinder and a sphere.

2.1 Flow Over a Cylinder

In the case of a circular cylinder of radius R, the velocity at the edge of the boundary-layer is a function of $\bar{x}$ $(= \frac{x}{R})$ given by

$$\frac{u_e(\bar{x})}{u_\infty} = 2\sin(\bar{x}), \qquad \bar{x} = \frac{x}{R}. \tag{5}$$

For the case of two-dimensional flows ($j = 0$), the expressions for ξ and β can be written as

$$\xi = 2(1-\cos\bar{x}), \qquad \beta(\bar{x}) = \frac{2\cos\bar{x}}{1+\cos\bar{x}}. \tag{6}$$

Using (5) and (6) in equation (3), we get

$$f_{\eta\eta\eta} + f f_{\eta\eta} + \beta(\bar{x})(1 - f_\eta^2) = 2B(\bar{x})(f_\eta f_{\eta\bar{x}} - f_{\eta\eta} f_{\bar{x}}), \tag{7}$$

where

$$B(\bar{x}) = \tan\left(\frac{\bar{x}}{2}\right).$$

The boundary conditions reduce to

$$f(\bar{x},0) = 0, \qquad f_\eta(\bar{x},0) = 0, \qquad f_\eta(\bar{x},\eta_\infty) = 1. \tag{8}$$

Equation (7) with conditions (8) has been solved numerically with the known pressure distribution $\beta(\bar{x})$ (see equation (6)) using an implicit finite difference scheme in combination with the quasilinearization technique ([6],[7]). For the sake of completeness a brief description is given here. The nonlinear partial differential equation (7) is replaced by a sequence of linear partial differential equations using quasilinearization technique. Then, the resulting sequence of linear partial differential equations is expressed in difference form using central difference scheme in η-direction and backward difference scheme in $\bar{x}$- direction. In each iteration step, the difference equations were then reduced to a system of linear algebraic equations with a tri-diagonal structure which is solved using Thomas algorithm (see [8]). A convergence criterion based on the relative difference between the current and the previous iterations has been used. When this difference becomes less than 10^{-4}, the solution is assumed to have converged and the iterative process is terminated. The wall shear stress distribution $f_{\eta\eta}(\bar{x}, 0)$ along the body surface in the streamwise direction has been computed and can be represented by the interpolating polynomial function $f_{\eta\eta}(\bar{x}, 0)$ using MATLAB as:

$$\begin{aligned} f_{\eta\eta}(\bar{x}, 0) = & -2.6462\bar{x}^{10} + 23.9121\bar{x}^{9} - 92.2977\bar{x}^{8} + 198.3232\bar{x}^{7} - 259.2157\bar{x}^{6} \\ & + 211.3968\bar{x}^{5} - 106.0527\bar{x}^{4} + 3.09092\bar{x}^{3} - 4.7408\bar{x}^{2} + 0.2643\bar{x}^{1} + 1.2310. \end{aligned} \tag{9}$$

The result given by equation (9) is used as an input data while solving the corresponding inverse problem in the next section. The accuracy in approximating the interpolating polynomial function $f_{\eta\eta}(\bar{x}, 0)$ as compared to the exact numerical results $f_{\eta\eta}(\bar{x}, 0)$ is displayed in Figure 2.

2.2 Flow Over a Sphere

In the case of a sphere of radius R, the free stream velocity distribution is given by (see [9])

$$\frac{u_e(\bar{x})}{u_\infty} = \frac{3}{2}\sin\bar{x}, \qquad \frac{r}{R} = \sin\bar{x}, \qquad \bar{x} = \frac{x}{R}. \tag{10}$$

For the axi-symmetric flow case ($j = 1$), the expressions for ξ and β are given by

$$\xi = \frac{1}{2}(1-\cos\bar{x})^2(2+\cos\bar{x}), \quad \text{and} \quad \beta(\bar{x}) = \frac{2\cos\bar{x}(2+\cos\bar{x})}{3(2+\cos\bar{x})^2}. \tag{11}$$

As in the case of a cylinder, in the case of a sphere using (10) and (11) in equation (3), we get equation (7) and boundary conditions (8), where the expressions for $\beta(\bar{x})$ and $B(\bar{x})$ are now given by

$$B(\bar{x}) = \frac{\tan(\frac{\bar{x}}{2})(2+\cos(\bar{x}))}{3(1+\cos(\bar{x}))}, \quad \text{and} \quad \beta(\bar{x}) = \frac{2\cos\bar{x}(2+\cos\bar{x})}{3(2+\cos\bar{x})^2}. \tag{12}$$

Similar to the case of a cylinder, equation (7) with the conditions (8) has been solved numerically using an implicit finite difference scheme in combination with the quasilinearization

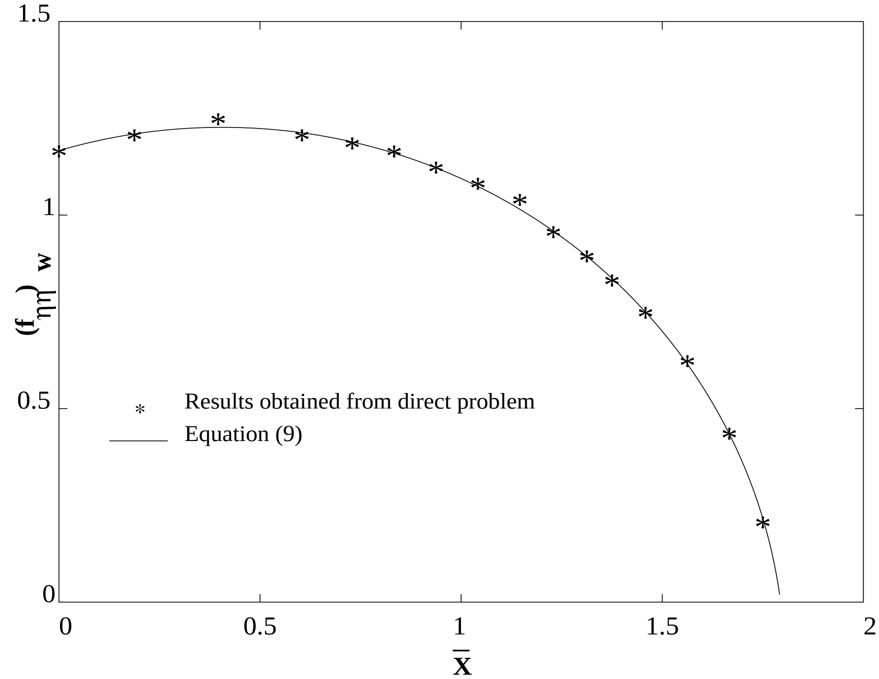

Figure 2: Comparisons of the interpolating polynomial $f_{\eta\eta}(\bar{x}, 0)$ with the exact numerical data (cylinder)

technique for the known pressure distribution $\beta(\bar{x})$ and the function $B(\bar{x})$ given by equation (12). Finally, the wall shear distribution, $f_{\eta\eta}(\bar{x}, 0)$ along the surface of the sphere in the streamwise direction has been computed and represented by the interpolating polynomial function $f_{\eta\eta}(\bar{x}, 0)$ using MATLAB as

$$\begin{aligned} f_{\eta\eta}(\bar{x}, 0) = &- 1.5129 * 10^2\bar{x}^{15} + 2.2681 * 10^3\bar{x}^{14} - 1.5317 * 10^4\bar{x}^{13} + 6.1578 * 10^4\bar{x}^{12} \\ &- 1.6407 * 10^5\bar{x}^{11} + 3.0524 * 10^5\bar{x}^{10} - 4.0689 * 10^5\bar{x}^{9} + 3.9243 * 10^5\bar{x}^{8} \\ &+ 1.3523 * 10^5\bar{x}^{6} + 4.632 * 10^4\bar{x}^{5} + 1.0468 * 10^4\bar{x}^{4} - 1.4422 * 10^3\bar{x}^{3} \\ &- 2.7313 * 10^5\bar{x}^{7} + 1.0492 * 10^2\bar{x}^{2} - 2.9142\bar{x} + 0.92947. \end{aligned} \tag{13}$$

For the case of sphere, $f_{\eta\eta}(\bar{x}, 0)$ given by equation (13) is also used as an input data while solving the corresponding inverse problem in section 3. The accuracy in approximating the interpolating polynomial function $f_{\eta\eta}(\bar{x}, 0)$ as compared to the exact data $f_{\eta\eta}(\bar{x}, 0)$ is displayed in Figure 3.

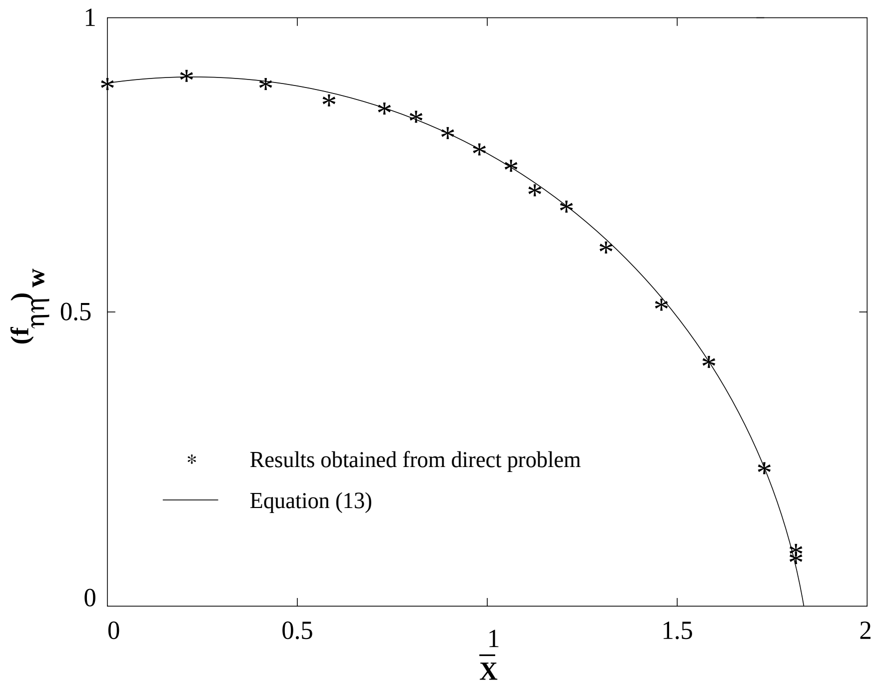

Figure 3: Comparisons of the interpolating polynomial $f_{\eta\eta}(\bar{x}, 0)$ with the exact numerical data (sphere)

3 Inverse Problems

In this section, we confine attention on inverse problems in steady incompressible boundary layer flows past a cylinder and a sphere with known wall shear stress distributions which are obtained as solutions of the direct problems (see section 2).

3.1 Flow Past a Cylinder

The governing equation and boundary conditions for boundary-layer flow past a cylinder can be written in dimensionless form as

$$f_{\eta\eta\eta} + f f_{\eta\eta} + \beta(1 - f_\eta^2) = 2B(\bar{x})(f_\eta f_{\eta\bar{x}} - f_{\eta\eta} f_{\bar{x}}), \tag{14}$$

$$f(\bar{x}, 0) = 0, \qquad f_\eta(\bar{x}, 0) = 0, \qquad f_\eta(\bar{x}, \eta_\infty) = 1, \tag{15}$$

where $B(\bar{x}) = \tan(\frac{\bar{x}}{2})$, $\bar{x} = \frac{x}{R}$ and the unknown function $\beta(\bar{x})$ to be determined by inverse calculation procedure. For inverse boundary-layer calculations the wall shear distribution along the surface of the cylinder in the streamwise direction, obtained as a solution of direct problem, (in section 2.1) is written as

$$\begin{aligned} f_{\eta\eta}(\bar{x},0) =& -2.6462\bar{x}^{10} + 23.9121\bar{x}^{9} - 92.2977\bar{x}^{8} + 198.3232\bar{x}^{7} - 259.2157\bar{x}^{6} \\ &+ 211.3968\bar{x}^{5} - 106.0527\bar{x}^{4} + 3.09092\bar{x}^{3} - 4.7408\bar{x}^{2} + 0.2643\bar{x}^{1} + 1.2310. \end{aligned} \tag{16}$$

Here $f_{\eta\eta}(\bar{x},0)$ is prescribed as a boundary condition for the equation (14) along with the other three boundary conditions given by equation (15). In inverse boundary-layer calculation procedure by invariant imbedding technique, these four boundary conditions correctly determine the unknown pressure distribution $\beta(\bar{x})$ in the third order equation (14).

The range of integration with respect to $\bar{x}$ is divided into a suitable number of intervals and derivatives with respect to $\bar{x}$ are approximated by two-point backward differences, resulting in the following third order nonlinear ordinary differential equation at streamwise station $\bar{x} = \bar{x}_n$

$$f_{\eta\eta\eta} + f f_{\eta\eta} + \beta(1 - f_{\eta}^{2}) = 2\frac{B(\bar{x})}{\triangle\bar{x}}\{f_{\eta}(f_{\eta} - f_{\eta}(\bar{x}_{n-1})) - f_{\eta\eta}(f - f(\bar{x}_{n-1}))\}, \tag{17}$$

where $f = f(\bar{x}_n, \eta)$, $f(\bar{x}_{n-1}) = f(\bar{x}_{n-1}, \eta)$, $B(\bar{x}) = B(\bar{x}_n)$ and $\beta = \beta(\bar{x}_n)$. This nonlinear equation is solved by iteration. At first, the nonlinear ordinary differential equation (17) is being linearized with respect to a previous iterate values by the method of quasilinearization [7]. This technique is used to linearize the momentum equation (17) with respect to $(f^o, f^o_{\eta}, f^o_{\eta\eta}, f^o_{\eta\eta\eta}, \beta^o)$ as

$$f_{\eta\eta\eta} + X_1^o f_{\eta\eta} + X_2^o f_{\eta} + X_3^o f + X_4^o \delta\beta = X_5^o, \tag{18}$$

where unsuperscripted quantities are current iterates and superscripted quantities are interms of previous iterative values. The coefficients in equation (18) are given by

$$\begin{aligned} X_1^o &= f + 2\frac{B(\bar{x}_n)}{\triangle\bar{x}}(f - f(\bar{x}_{n-1})), \\ X_2^o &= -2\left(\beta^o + \frac{B(\bar{x}_n)}{\triangle\bar{x}}\right) f_{\eta} - 2\frac{B(\bar{x}_n)}{\triangle\bar{x}}(f_{\eta} - f_{\eta}(\bar{x}_{n-1})), \\ X_3^o &= \left(1 + 2\frac{B(\bar{x}_n)}{\triangle\bar{x}}\right) f_{\eta\eta}, \\ X_4^o &= 1 - f_{\eta}^2, \\ X_5^o &= -\beta^o - \left(\beta^o + 2\frac{B(\bar{x}_n)}{\triangle\bar{x}}\right) f_{\eta}^2 + \left(1 + 2\frac{B(\bar{x}_n)}{\triangle\bar{x}}\right) f f_{\eta\eta}, \\ \delta\beta &= \beta - \beta^o. \end{aligned}$$

Equation (18) is now rewritten as a system of equations as

$$\left.\begin{aligned} Z_1' &= Z_2, \\ Z_2' &= Z_3, \\ Z_3' &= X_5^o - (X_1^o Z_3 + X_2^o Z_2 + X_3^o Z_1 + X_4^o \delta\beta), \end{aligned}\right\}, \tag{19}$$

where $Z_1 = f$, $Z_2 = f_\eta$ and $Z_3 = f_{\eta\eta}$. Here, wall shear stress is known and so equation (19) is a two-point boundary value problem containing unknown parameter $\delta\beta$ with boundary conditions

$$Z_1(0) = Z_2(0) = 0, \qquad Z_3(0) = f_{\eta\eta}(\bar{x}, 0), \qquad \text{and} \qquad Z_2(\eta_\infty) = 1, \tag{20}$$

where $f_{\eta\eta}(\bar{x}, 0)$ is given by equation (16) and η_∞ is the edge of the boundary-layer and it is sufficiently far from the surface for the asymptotic condition ($Z_2(\eta_\infty) = 1$) to be applied without significant error. This two-point boundary value problem is transformed into a pair of initial value problems using invariant imbedding approach (which is based on the Ricatti transformation). Although the inverse problem is not amenable to this approach in the basic form of equation (19), a suitable form is obtained by following changes of variables which is a key step in the invariant imbedding approach [3]. The unknown parameter $\delta\beta$ is linearly combined with the highest derivative of f (i.e, Z_3) to form a new variable

$$Z_4 = Z_3 + C\delta\beta, \tag{21}$$

where the constant C may be arbitrarily chosen. Here C is taken as -1, *i.e.*

$$Z_4 = Z_3 - \delta\beta. \tag{22}$$

Substituting equation (22) into equation (19), we get the system of equations as:

$$\left.\begin{aligned} Z_1' &= Z_2, \\ Z_2' &= Z_3, \\ Z_3' &= X_5^o - ((X_1^o + X_4^o) Z_3 + X_2^o Z_2 + X_3^o Z_1 - X_4^o Z_4), \\ Z_4' &= Z_3', \end{aligned}\right\}, \tag{23}$$

with the boundary conditions given by equation (20). The invariant imbedding transformation is now carried out as follows. Homogeneous and inhomogeneous invariant imbedding functions, u_i and w_i, are defined by

$$Z_i = u_i Z_4 + w_i, \qquad i = 1, 2, 3 \tag{24}$$

Then the following system of equations for the invariant imbedding functions is obtained

$$\left.\begin{aligned} u_1' &= u_2 + R_1 u_1, \\ u_2' &= u_3 + R_1 u_2, \\ u_3' &= R_1(u_3 - 1), \end{aligned}\right\}, \tag{25}$$

$$\left.\begin{aligned} w_1' &= w_2 + R_2 u_1, \\ w_2' &= w_3 + R_2 u_2, \\ w_3' &= R_2(u_3 - 1), \end{aligned}\right\}, \tag{26}$$

where

$$R_1 = (X_1^o + X_4^o)u_3 + X_2^o u_2 + X_3^o u_1 - X_4^o, \qquad R_2 = (X_1^o + X_4^o)w_3 + X_2^o w_2 + X_3^o w_1 - X_5^o.$$

The boundary conditions are transformed to

$$u_1(0) = u_2(0) = u_3(0) = w_1(0) = w_2(0) = 0, \qquad w_3(0) = f_{\eta\eta}(\bar{x}, 0). \tag{27}$$

Equations (25)-(26) with initial conditions (27) is an initial value problem which is solved using well known Runge-Kutta fourth order method. The invariant imbedding functions are stored at each point and for efficiency, the nonlinear system of equations (25) is solved independently. Next, the linear system of equations (26) is solved separately. The invariant imbedding function values are used to find outer boundary condition for Z_4

$$Z_4(\eta_\infty) = \frac{1 - w_2(\eta_\infty)}{u_2(\eta_\infty)},$$

and also

$$\delta\beta = Z_4(\eta_\infty)\{u_3(\eta_\infty) - 1\} + w_3(\eta_\infty).$$

Later, inward integration from $\eta = \eta_\infty$ to $\eta = 0$ is carried out to obtain Z_4 for the initial value problem

$$Z_4' = -(R_1 Z_4 + R_2), \qquad Z_4(\eta_\infty) = \frac{1 - w_2(\eta_\infty)}{u_2(\eta_\infty)}.$$

Finally, the original unknowns (Z_1, Z_2, Z_3) are computed algebraically from equations (22) and (24) as

$$\left.\begin{aligned} Z_3 &= Z_4 + \delta\beta, \\ Z_2 &= u_2 Z_4 + w_2, \\ Z_1 &= u_1 Z_4 + w_1. \end{aligned}\right\},$$

Numerical results for the pressure distribution $\beta(\bar{x})$ up to the point of separation obtained as solutions of the inverse problem (14)-(15) have been compared with the exact values of $\beta(\bar{x})(=\frac{2\cos\bar{x}}{1+\cos\bar{x}})$, used in direct problem in section 2.1 and the results are displayed in Table 1 as well as in Figure 4.

Table 1. Distribution of $\beta(\bar{x})$ over cylinder

$\bar{x}$	Present Results	Exact Results$\left(\beta(\bar{x})=\frac{2\cos\bar{x}}{1+\cos\bar{x}}\right)$
0.0	1.000300	1.000000
0.2	0.987065	0.989932
0.4	0.953392	0.958908
0.6	0.907935	0.904311
0.8	0.823038	0.821245
1.0	0.709820	0.701553
1.2	0.530020	0.531956
1.4	0.295660	0.290550
1.6	-0.061697	-0.060155
1.8	-0.592398	-0.587998

Figure 4 shows clearly a gradual decrease of $\beta(\bar{x})$ as $\bar{x}$ increases from zero to point of separation. It is observed from Table 1 that the present invariant imbedding approach recovers the values of pressure distributions $\beta(\bar{x})$ with 1% error when it is compared with the exact values of pressure distribution $\beta(\bar{x})(=\frac{2\cos\bar{x}}{1+\cos\bar{x}})$.

It may be remarked that Keller and Cebeci [1] have presented the solutions of inverse problem in the study of the boundary-layer equations for laminar two-dimensional flow using a finite difference method [1]. Later, Horton [2] describes an alternative numerical procedure for solving the same inverse problem and compared his results with the results of Keller and Cebeci [1]. In order to verify the accuracy of the present invariant imbedding approach, the pressure gradient distributions $\beta(\xi)$ have been computed for the following wall shear distributions

$$(i)\ f_{\eta\eta}(\xi,0)=0.46960(1-\xi), \tag{28}$$

$$(ii)\ f_{\eta\eta}(\xi,0)=0.46960(1-\xi)(1-0.526490\xi), \tag{29}$$

up to the point of separation and compared the results with those of Keller and Cebeci [1] and Horton [2]. Some of the comparisons of the present results are displayed in Table 2

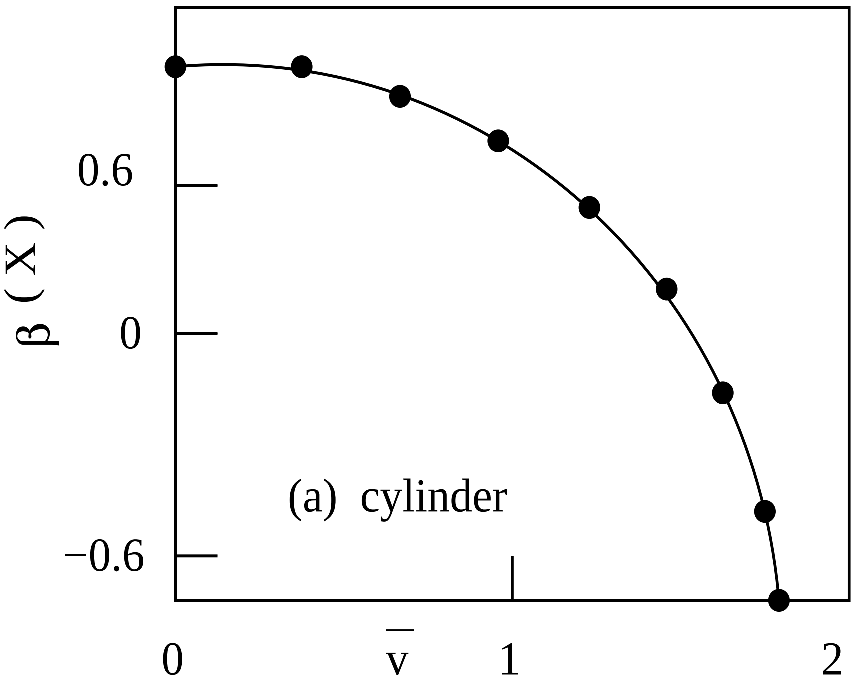

Figure 4: Distribution of pressure gradient parameter ($\beta(\bar{x})$) for cylinder ——— present results, ● exact values used in the direct problem

and they are found to be in a good agreement with the available results which validate the present scheme of inverse boundary-layer computations.

Table 2 Comparison of pressure distribution ($\beta(\bar{x})$)

$\bar{x}$	Present Results for Eq.(28)	Horton [2] for Eq.(28)	Keller and Cebeci [1] for Eq.(28)	Presents results for Eq.(29)	Horton [2]] for Eq.(29)
0.00	0.000000	0.00000	-0.00003	0.0	0.0
0.20	-0.084218	-0.08432	-0.08424	-0.104446	-0.10
0.40	-0.154206	-0.15436	-0.15418	-0.185953	-0.18
0.60	-0.207569	-0.20776	-0.20747	-0.229333	-0.22
0.80	-0.239012	-0.23949	-0.23940	-0.242863	-0.24
0.90	-0.243697	-0.24349	-0.24376	-0.241444	-0.24
0.95	-0.241884	-0.24088	–	-0.238975	-0.23
1.00	-0.233832	-0.23353	–	-0.221529	-0.22

3.2 Flow Past a Sphere

The governing equation and boundary conditions for boundary-layer flow past a sphere can be written in dimensionless form as

$$f_{\eta\eta\eta} + ff_{\eta\eta} + \beta(1 - f_\eta^2) = 2B(\bar{x})(f_\eta f_{\eta\bar{x}} - f_{\eta\eta} f_{\bar{x}}), \tag{30}$$

$$f(\bar{x}, 0) = 0, \qquad f_\eta(\bar{x}, 0) = 0, \qquad f_\eta(\bar{x}, \eta_\infty) = 1, \tag{31}$$

where $\bar{x} = \frac{x}{R}$, $\frac{r}{R} = \sin\bar{x}$ and $B(\bar{x}) = \frac{\tan(\frac{\bar{x}}{2})(2+\cos(\bar{x}))}{3(1+\cos(\bar{x}))}$.

The inverse boundary-layer computation procedure has been implemented for boundary-layer flow past a sphere with known wall shear distribution $f_{\eta\eta}(\bar{x}, 0)$ (obtained as a solution of the direct problem in section 2.2) given by

$$\begin{aligned} f_{\eta\eta}(\bar{x}, 0) = & - 1.5129 * 10^2 \bar{x}^{15} + 2.2681 * 10^3 \bar{x}^{14} - 1.5317 * 10^4 \bar{x}^{13} + 6.1578 * 10^4 \bar{x}^{12} \\ & - 1.6407 * 10^5 \bar{x}^{11} + 3.0524 * 10^5 \bar{x}^{10} - 4.0689 * 10^5 \bar{x}^9 + 3.9243 * 10^5 \bar{x}^8 \\ & + 1.3523 * 10^5 \bar{x}^6 + 4.632 * 10^4 \bar{x}^5 + 1.0468 * 10^4 \bar{x}^4 - 1.4422 * 10^3 \bar{x}^3 \\ & - 2.7313 * 10^5 \bar{x}^7 + 1.0492 * 10^2 \bar{x}^2 - 2.9142 \bar{x} + 0.92947. \end{aligned} \tag{32}$$

Similar to the case of a cylinder, in the case of a sphere the unknown pressure distribution $\beta(\bar{x})$ in the equation (30) can be obtained accurately using boundary conditions (31)-(32) with the help of invariant imbedding technique. Since the inverse solution procedure is described in great detail in the previous section 3.1, its detailed description is not presented here. Comparisons of the pressure distribution $\beta(\bar{x}) \left(= \frac{2\cos\bar{x}(2+\cos\bar{x})}{3(2+\cos\bar{x})^2}\right)$ up to the point of separation obtained as a solution of the inverse problem (30)-(32) with the exact values of $\beta(\bar{x})$ used in direct problem in section 2.2, are displayed in Table 3 as well as in Figure 5.

Table 3 Distribution of $\beta(\bar{x})$ over sphere

$\bar{x}$	Present Results	Exact Results $\left(\beta(\bar{x}) = \frac{2\cos\bar{x}(2+\cos\bar{x})}{3(1+\cos\bar{x})^2}\right)$
0.0	0.508121	0.500000
0.2	0.498413	0.496627
0.4	0.489311	0.486021
0.6	0.465192	0.466577
0.8	0.439610	0.435089
1.0	0.392803	0.385672
1.2	0.304181	0.307474
1.4	0.181901	0.179630
1.6	-0.036956	-0.040706
1.8	-0.438088	-0.449622

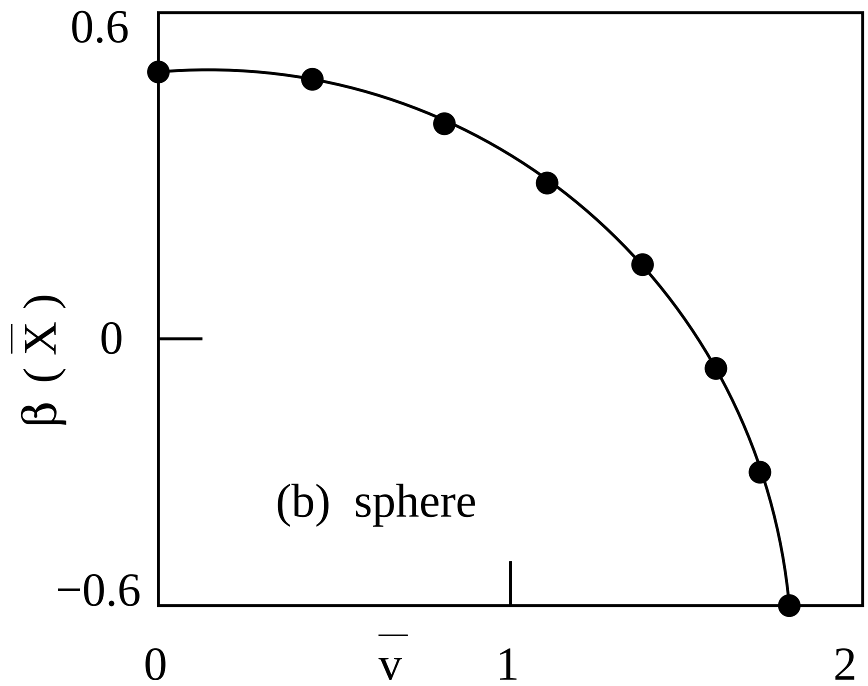

Figure 5: Distribution of pressure gradient parameter ($\beta(\bar{x})$) for sphere ——— present results, • exact values used in the direct problem

It is observed from Table 3 that the present invariant imbedding approach recovers the values of pressure distributions $\beta(\bar{x})$ with 1% error when it is compared with the exact values of pressure distribution $\beta(\bar{x})\left(=\frac{2\cos\bar{x}(2+\cos\bar{x})}{3(2+\cos\bar{x})^2}\right)$.

It is worth mentioning here that the change of variable defined by equation (21) in section 3.1 plays an important role in the present scheme as it allows to test the robustness of the method for various choices of the constant C in (21). The method has been experimented with different values of C and it is found that for large absolute values of C, it did not produce a well-conditioned invariant imbedding systems for our problem. Best solutions were obtained when $C \approx -1$. Therefore in our scheme here we have used this value of C in (21) resulting in equation (22).

4 Conclusions

An invariant imbedding approach for solving boundary-layer equations in inverse mode is presented. The implementation of the invariant imbedding approach for solving inverse problems in non-planar boundary-layer flows has been carried out on two test cases and the results are encouraging for further exploration of the method and its application to perhaps other types of flows such turbulent boundary-layer flows. This remains a topic of future research.

References

[1] Keller H. B., and Cebeci T., "An Inverse Problem in Boundary-Layer Flows: Numerical Determination of Pressure Gradient for a Given Wall Shear", *Jour. Comp. Phys.* **10** (1972), pp. 151-161.

[2] Horton H. P., "Seperating laminar boundary layers with prescribed wall shear", *AIAA J.* **12** (1974), pp. 1772-1774.

[3] Horton H. P., *Invariant imbedding algorithms for inverse boundary layer problems*, College Report No. QMW - EP - 1102, Queen Mary & Westfield College, University of London, U.K., 1994

[4] Daripa P., and Sirovich L., "An Inverse Method for Subcritical Flows", *Jour. Comp. Phys.* **63** (1986), pp. 311 - 328.

[5] Daripa P., An Exact Inverse Method for Subcritical Flows, *Quart. Appl. Math.* **XLVI** (1988), pp. 505 - 526.

[6] Stanley Lee E., *Quasilinearization and Invariant Imbedding*, Academic Press, New York, 1968.

[7] Inouye K., and Tate A., "Finite difference version of quasilinearization applied to boundary layer equations", *AIAA J.* **12** (1974), pp. 558 - 560.

[8] Lam Chung-Yau, *Applied numerical methods for partial differential equations*, Prentice Hall, New York, 1994.

[9] Schlichting H., *Boundary Layer Theory*, Springer-Verlag, 2000.